



Development of Ultra-High Molecular Weight Polyethylene (UHMWPE) Coating by Cold Spray Technique

Kesavan Ravi, Yuji Ichikawa, Tiana Deplancke, Kazuhiro Ogawa, Olivier Lame, and Jean-Yves Cavaille

(Submitted December 17, 2014; in revised form June 26, 2015)

Ultra-high molecular weight polyethylene or UHMWPE is an extremely difficult material to coat with, as it is rubbery and chemically very inert. The Cold Spray process appears to be a promising alternative processing technique but polymers are in general difficult to deposit using this method. So, attempts to develop UHMWPE coatings were made using a downstream injection cold spray technique incorporating a few modifications. A conventional cold spray machine yielded only a few deposited particles of UHMWPE on the substrate surface, but with some modifications in the nozzle geometry (especially the length and inner geometry) a thin coating of 45 μm on Al substrate was obtained. Moreover, experiments with the addition of fumed nano-alumina to the feedstock yielded a coating of 1-4 mm thickness on Al and polypropylene substrates. UHMWPE was seen to be melt crystallized during the coating formation, as can be seen from the differential calorimetry curves. Influence of nano-ceramic particles was explained by observing the creation of a bridge bond between UHMWPE particles.

Keywords coating, cold spray, nano-ceramic particle, ultra-high molecular weight polyethylene (UHMWPE)

1. Introduction

Polymer coatings have a strong variety of applications like surface protection from corrosion (Ref 1), protection from cavitation erosion or mechanical impacts (Ref 2), electronic applications (Ref 3), packaging (Ref 4), and biocompatible membrane (Ref 5) etc. The applications of coatings have greatly increased, largely driven by the competitive need to reduce costs, weight, and volume.

The aim of this study is to develop ultra-high molecular weight polyethylene (UHMWPE) coating by cold spray technique.

The high molecular weight provides exceptional physical and mechanical properties to UHMWPE. In particular, it has excellent wear resistance and is commonly used for total joint implants (Ref 6). It also has excellent resistance to impacts and is a material of choice for body armors (Ref 7). Its outstanding wear and impact resistance is related to its high ductility. It has a large elongation at break (typically several hundred percent) and, as a result, a great ability to absorb energy before fracture (Ref 8).

Kesavan Ravi, Yuji Ichikawa, and Kazuhiro Ogawa, Fracture and Reliability Research Institute, Tohoku University, 6-6-11-720, Aoba, Aramaki, Aoba-ku, Sendai 980-8579, Japan; and **Tiana Deplancke, Olivier Lame, and Jean-Yves Cavaille**, Materials Engineering and Science (MATEIS), CNRS, INSA-Lyon UMR5510, Université de Lyon, 69621 Villeurbanne, France. Contact e-mail: kesavan_ravi@rift.mech.tohoku.ac.jp.

Nomenclature

Gwt. %	Weight percentage of guest particles
D	Average diameter of host particle (m)
d	Average diameter of guest particles (m)
ρ_D	Density of host particles (kg/m^3)
ρ_d	Density of the guest particles (kg/m^3)
ΔE	Energy required for melting one particle ($\text{kg m}^2/\text{s}^2$)
ΔH	Melting enthalpy of the crystal (m^2/s^2)
X_c	Crystallinity of the nascent powder
C_p	Heat capacity ($\text{m}^2/\text{s}^2/\text{K}$)
m	Mass of the UHMWPE particle (kg)
r	Radius of the UHMWPE particle (m)
E_c	Kinetic energy of the UHMWPE particle ($\text{kg m}^2/\text{s}^2$)
V	Velocity of the UHMWPE particle (m/s)
ΔT	Temperature change (K)

UHMWPE is semi-crystalline in nature and the powder used in this study, has a molecular weight of 10.5 mg/mol. The presence of both crystal network and the entanglements of the polymeric chains characterize the semi-crystalline nature of the UHMWPE polymer. The high molecular weight of UHMWPE leads the material to exhibit a broad rubbery plateau unlike the other lower molecular weight polymers. Figure 1 shows the comparison of the rubbery plateau area in the case of normal PE and UHMWPE. As a conclusion, UHMWPE in the temperature range of 150-300 $^{\circ}\text{C}$ is in melt state but exhibits elastic properties like rubber.

Since the high molecular weight of UHMWPE exhibits a very high viscosity in the melt region, it is not possible to

process by conventional techniques such as injection molding or extrusion. Special fabrication techniques like compression molding or sintering is used, at present, to process UHMWPE (Ref 8). In the case of non-planar surfaces, however, sintering compression is difficult to use on a large scale. The cold spray technique is for this reason investigated as a potential technique for coating UHMWPE onto different materials. Another advantage of the Cold Spray process would be its lower time and energy consumption.

The process of cold spraying (CS) involves the impact of powder particles on to a target at very high speeds to form coatings or solid components. It was originally developed in the mid-1980s at the Institute of Applied Mechanics of the Siberian Branch of the Russian Academy of Science (ITAM SB RAS) in Novosibirsk by Papyrin and co-workers (Ref 9) for metallic powders. The accelerating gas may be heated, mainly to achieve higher particle velocities. The powder particles, usually in the particle size range from 5 to 100 μm are accelerated by injection into a high velocity stream of gas. The high velocity gas is generated through the expansion of a pressurized preheated gas, which is accelerated to supersonic velocity, with an accompanying decrease in pressure and temperature, through a converging-diverging nozzle (Ref 10-12). The accelerated particles are then impacted onto the substrate after exiting the nozzle.

The major advantage of the cold spray process, which makes it attractive, is that, it is a solid-state process, which results in many unique and high-quality coating characteristics. The deposition on the surface is purely attributed to the plastic deformation of the particles. Cold spray process offers several advantages like high deposition efficiency and deposition rate, flexibility of substrate-coating selection, no or little masking etc. Most importantly, the cold spray employs low temperature gas due to which there is no risk of oxidation, thermal degradation, and grain growth or phase transformation. Additionally, the high temperature effects on the substrate are also avoided.

It is worthy to be noted that only a very few works were performed with polymer particles in thermal spray/cold spray (Ref 13-17).

The paper is devoted to an investigation of the development and characterization of UHMWPE coatings by cold spray technique.

2. Experimental

2.1 Cold Spray

The UHMWPE powder was deposited on each substrate using downstream injection cold spray technique. It is a conventional low-pressure downstream injection cold spray instrument available under the name Dymet 403J (Obninsk Center for Powder Spraying (OCPS), Russia). Figure 2 shows the schematic of the downstream injection cold spray apparatus used in the experiment. Pressurized gas (air) from 0.2 to 0.8 MPa was supplied from a

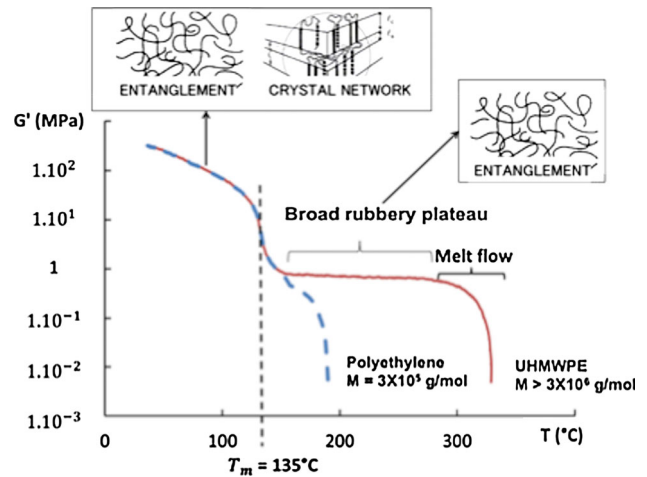


Fig. 1 Relationship between strength of UHMWPE and temperature (Ref 8)

compressor, which meets the powder particles at the nozzle region. The gas temperature can be varied from room temperature to 500 $^{\circ}\text{C}$. The powder particles were fed from a vibrated powder feeder at a steady controllable rate. Feed rate was not calculated as a vibratory feeder was used. The air stream was passed through a de Laval nozzle. The polymer powder is fed after the de Laval section. The air stream containing the polymer particles finally goes through a 100-mm-long diverging nozzle before hitting the Aluminum (Al) and Polypropylene (PP) substrates. The nozzle was held at right angles to the target with a standoff distance varied from 5 to 20 mm. Table 1 specifies the unit specification of the system.

To control the standoff distance between the nozzle and substrate surface and also to control the traverse parameters, the cold spray unit was mounted on a XYZ stage and manipulated by a personal computer. Figure 3 shows the photograph of the experimental setup.

2.2 Ultra-High Molecular Weight Polyethylene: Structural and Physical Characterization

UHMWPE used in this study is GUR 4170 obtained from Ticona (Oberhausen, Germany). It is in the form of powder with an average size distribution of 60 μm . Figure 4 shows the SEM image of the UHMWPE powder used in this study. The molecular mass deduced from viscosity measurements is 10.5 mg/mol. The crystallinity ratio was measured by differential scanning calorimetry (DSC) using a Rigaku apparatus at a heating rate of 10 $^{\circ}\text{C}/\text{min}$. The temperature and heat flow scales were calibrated using high purity alumina.

The nascent powder, rebound particles, and the deposited particles were analyzed by the DSC (Rigaku Thermo plus EVO2) to understand the difference in their thermal history. The rebound particles were collected after the cold spray. On the other hand, the deposited particles on Al and PP substrates were scraped off from the coatings to be analyzed. The reference material used in the analysis was Al_2O_3 , which was also used to calibrate

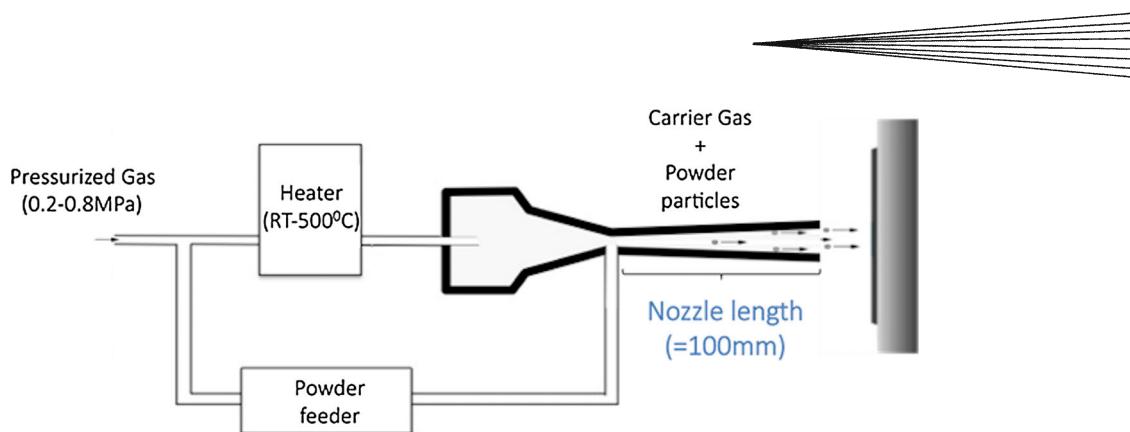


Fig. 2 A schematic of a typical downstream injection cold spray system

Table 1 Dymet 403j specifications

Parameter	Description
Power	220 V, 3.3 kW
Pressure of consumed air	0.2-1.0 MPa
Consumption of compressed air	0.4 m ³ /min
Temperature range	Room temperature—500 °C (5 modes)
Number of powder feeders	3

the instrument. The polymer samples were heated at a heating rate of 10 °C/min in the range of temperature 70-200 °C, and the subsequent DSC curve was plotted.

The morphological investigations were performed using a Hitachi SU-70, a field emission scanning electron microscope (FE-SEM), operated at 20 kV. A thin Platinum coating was applied prior to SEM observation by ion sputtering.

3. Results and Discussion

3.1 Cold Spray Experiments

3.1.1 Conventional Cold Spray Technique. A conventional downstream injection cold spray, with the specifications mentioned in the experimental section, was used to spray UHMWPE particles to see the possibility of the deposition. No noticeable deposition was observed after the spraying. Very few particles deposited on the surface of Al and heavy erosion was observed on PP substrate. Figure 5(a) shows the SEM image of a deposited UHMWPE particle on Al substrate. As can be seen from the Fig. 5(a), a lot of cracks were observed at the base of the UHMWPE particles after the impact. According to Assadi et al., the metallic particles, during a cold spray process, suffer a severe plastic deformation on impact with a substrate (Ref 18). The severe plastic deformation during the impact helps the metallic particles to create new active surface and bond with the substrate.

In the case of UHMWPE particles, however, instead of generating active surfaces by plastic deformation, the new surface creation was observed via crack generation leading

to a lack of high-energy surface and a decreased tendency of UHMWPE surface to bond with the substrate surface.

3.1.2 Cold Spray with a Long Nozzle. In order to generate new useful active surface area on impact, plastic deformation of the UHMWPE particles was essential. The plastic deformability of the polymer particle is known to increase with thermal softening (Ref 19). Thus, the increase of this effect was investigated.

The particles experience acceleration and heating during their traverse along the nozzle. Hence, for short nozzle length, the UHMWPE particles traveled with the carrier gas for a very short time. This led to low thermal softening of the particles. Alhulaifi et al. suggested that a low impact velocity and a moderately high particle temperature were desirable for the deposition of polymeric powder (Ref 20). One of the options to achieve a lower particle velocity and high particle temperature was to reduce the stagnation pressure and keep the stagnation temperature high. But, due to technical difficulties, the gas does not heat up when stagnation pressure is reduced more than 0.2 MPa. Hence, a nozzle arrangement was prepared (Fig. 6) that has a step in the flow, which would help in creating a shock at the center (as shown in Fig. 7). Such a shock would help in decelerating the gas/particles. An arrangement this way would help in increasing the static gas temperature and an increase in residence time of the particles during the flow. So, two diverging nozzles of 100 mm were attached to each other as shown in Fig. 6.

Consequently, downstream injection cold spray apparatus equipped with this nozzle was used to spray UHMWPE onto Al and PP substrates. Figure 6(a) and (b) shows the photographs of the short nozzle and the long nozzle, respectively, used in this study. Figure 7 represents the schematic of the inner geometry of the nozzles shown in Fig. 6.

Gas temperature and pressure range of 350-380 °C and 0.3-0.4 MPa, respectively, yielded a thin-layered UHMWPE coating of approximately 45 μm on Al substrate. Since, the average particle size of the UHMWPE was 60 μm, it was assumed that the coating obtained is a mono-particle layer. Figure 8 shows the image of the coated UHMWPE particle on Al substrate. A non-uniform deposition of the particles gives rise to the coloration as seen in the top view of the coating. Erosion of the

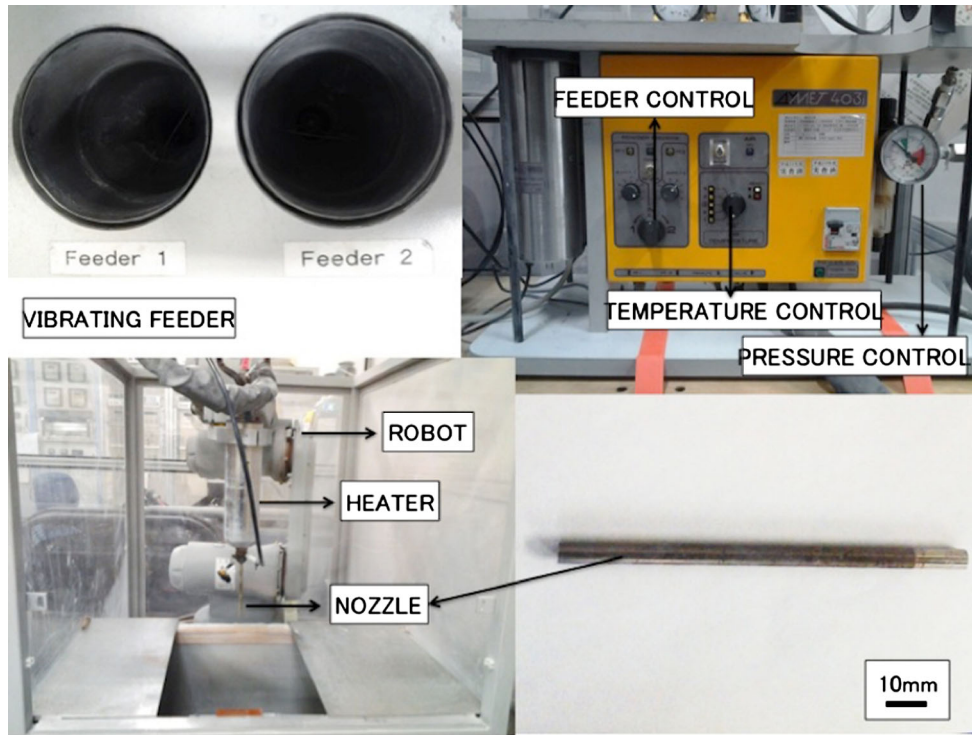


Fig. 3 Photograph of the experimental setup

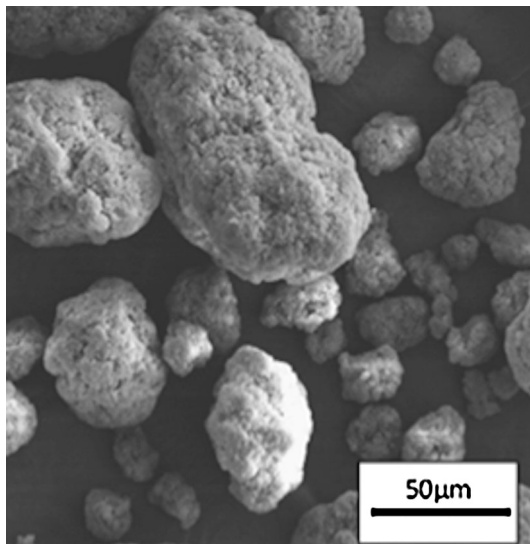


Fig. 4 SEM image of the UHMWPE

substrate was observed in the case of PP at all the temperature and pressure conditions tested.

A major difficulty observed in this case was that, even after 10 successive passes, the buildup in the coating thickness was not observed. It was seen that after the first layer formation, the particles tend to rebound from the surface. This suggests that the UHMWPE particle/particle

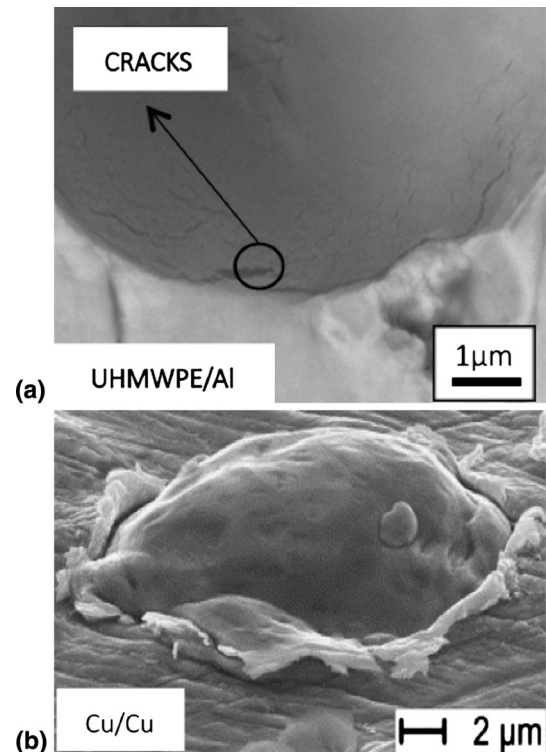


Fig. 5 (a) SEM image of UHMWPE particle deposited on Al substrate. (b) SEM image of Cu particle deposited on Cu substrate (Ref 18)

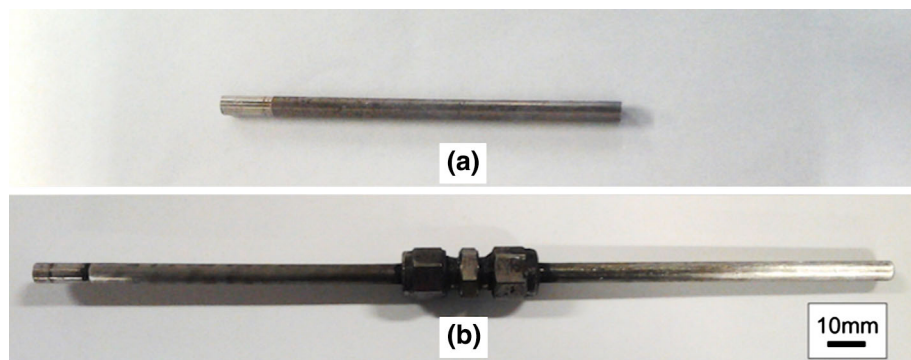


Fig. 6 Photograph of short nozzle (nozzle 1) and long nozzle (nozzle 2)

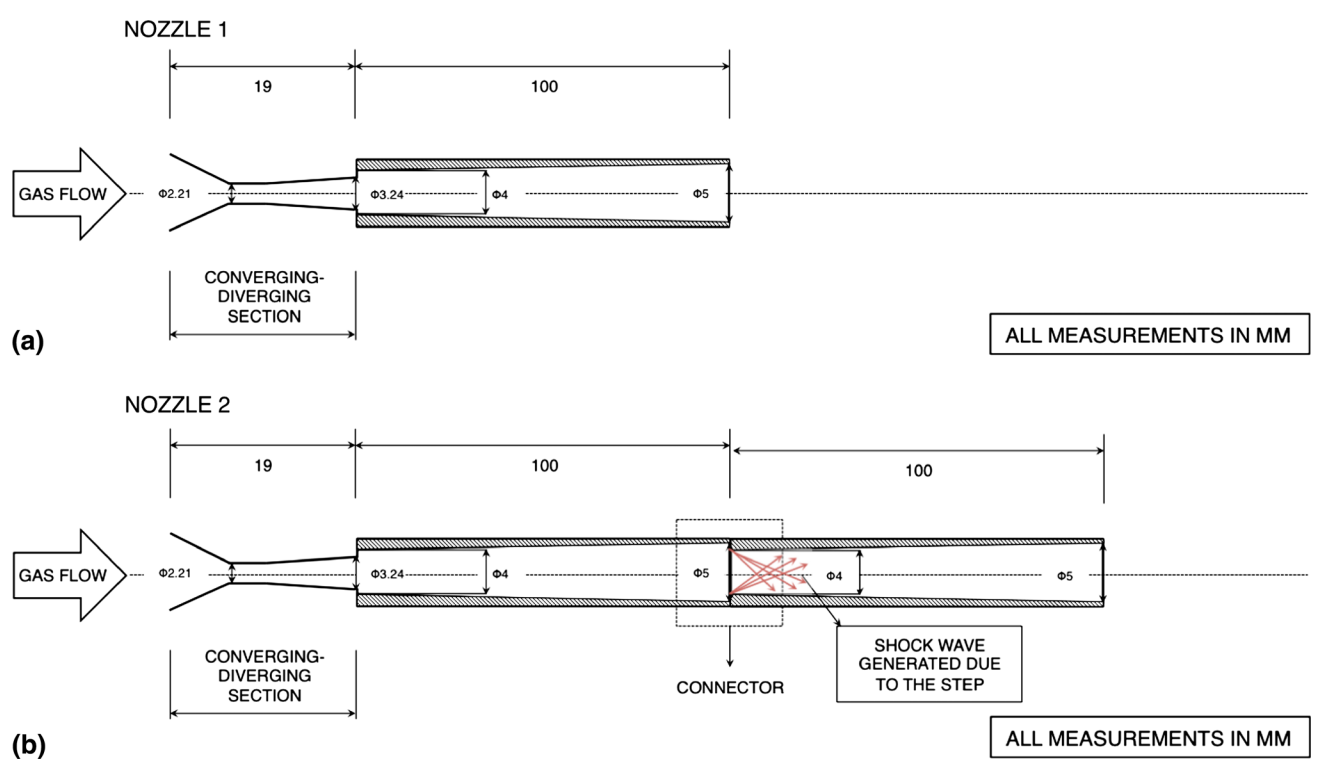


Fig. 7 (a) Schematic of the inner geometry of the short nozzle (nozzle 1). (b) Schematic of the inner geometry of the long nozzle (nozzle 2)

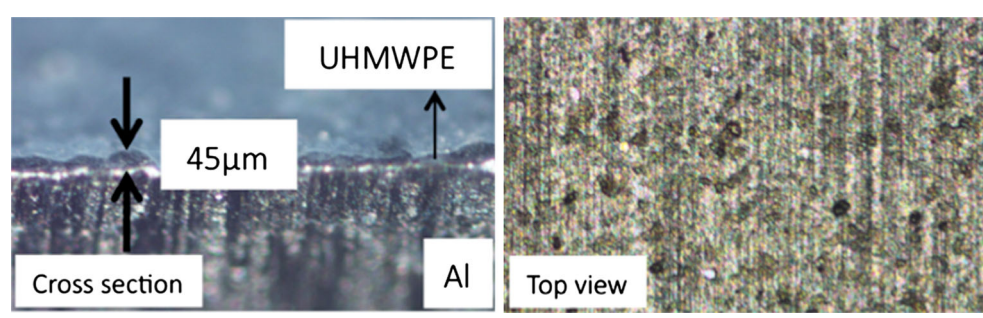


Fig. 8 Microscopic images of the UHMWPE coating on Al substrate

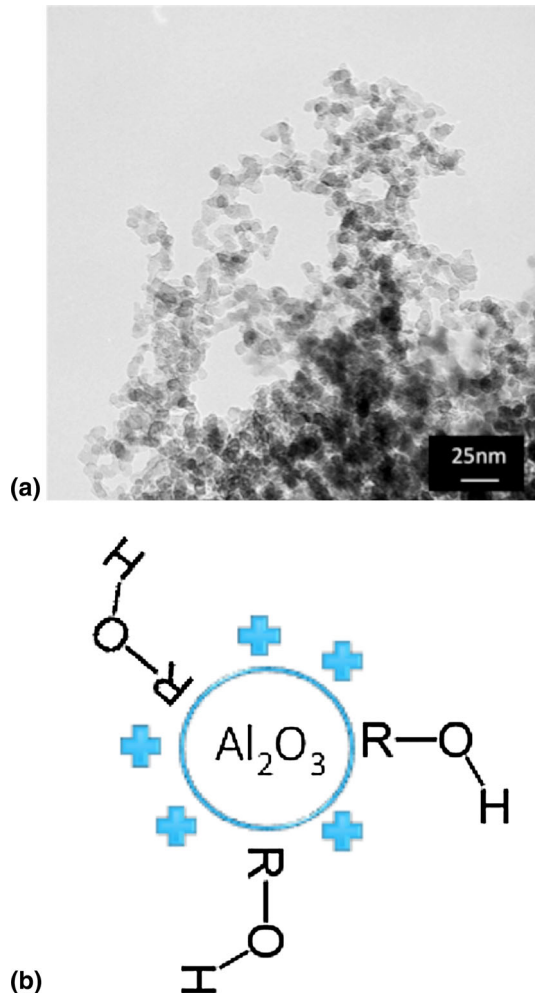


Fig. 9 (a) TEM image of Fumed nano-alumina used in this study. (b) Illustration showing the surface charge and hydroxyl groups on the surface of the fumed nano-alumina particle

bonding was not strong enough to increase the coating thickness. The other possibility is that the first layer induced an elastic rebound for the incoming second particles.

The surface energy and the wettability of a polymer depends, to a great extent, on the presence of hydrophilic groups such as ether, ester, and carboxyl groups (Ref 21). Generally the adhesion increases with the presence of hydrophilic groups so that a high surface energy is correlated to good adhesion. However, UHMWPE is a hydrophobic material (due to be presence of only C-H and C-C bonds). Hence, the UHMWPE particle/particle adhesion was expected to be low.

3.1.3 Cold Spray with the Addition of Nanoparticles. In this section, modification the surface of the UHMWPE particle in order to increase the bonding strength among the UHMWPE-UHMWPE particles was considered by adding Nano-alumina as an external binding agent. High surface area of these particles also contributes to the quality of the contact between particles.

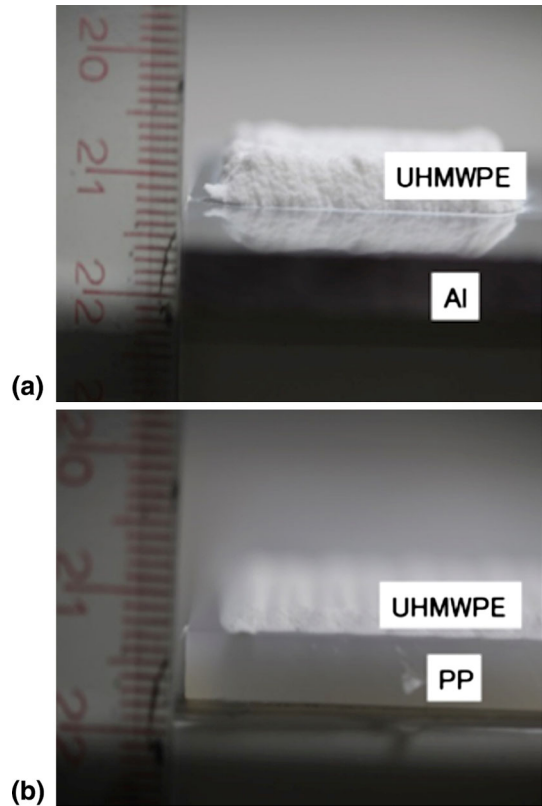


Fig. 10 (a) Photograph of the UHMWPE-fumed nano-alumina coating on Al. (b) Photograph of the UHMWPE-fumed nano-alumina coating on PP

Hence, the nano-alumina particles were expected to increase the stickiness of the UHMWPE particles.

Nano-alumina particles are well known polymer filler material and they are present in many of the polymer-nano composites. As far as thermoplastic matrices are concerned, addition of fillers has also been found to improve some mechanical properties, such as Young's modulus, fracture strength, and friction and wear behavior (Ref 22, 23), as well as thermal stability (Ref 24).

In this experiment, 4% of fumed nano-alumina powder (obtained from Evonik Industries) was hand mixed with the UHMWPE powder before the feeding process. The percentage by mass of nanoparticles used in the experiment is calculated based on the assumption of 100% surface coverage of the UHMWPE particles with a monolayer of alumina particles. It is assumed that all guest particles are of same size, and both the host and the guest particles are spherical (Ref 25). Based on these assumptions, the weight percentage of guest particles (Gwt.%) for 100% surface coverage is

$$\text{Gwt.}\% = \frac{(Nd^3\rho_d)}{(D^3\rho_D) + (Nd^3\rho_d)} \times 100 \quad \text{with}$$

$$N = \frac{4(D+d)^2}{d^2} \approx 4\left(\frac{D}{d}\right)^2,$$

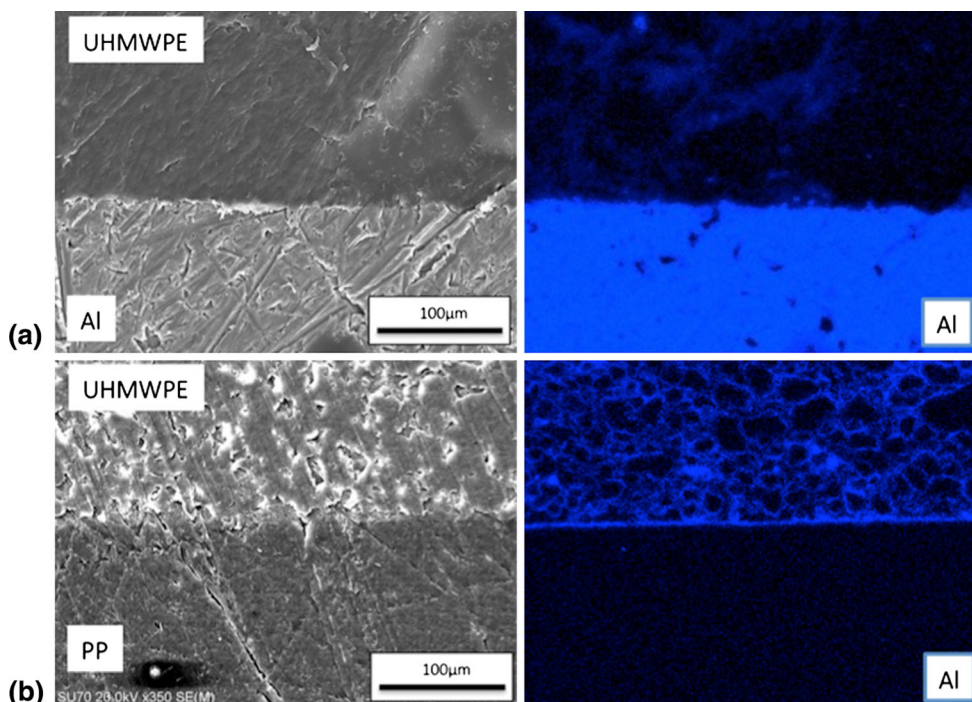


Fig. 11 (a) Cross-sectional SEM/EDX image of the coating on Al. (b) Cross-sectional SEM/EDX image of the coating on PP

where D is the average diameter of host particle, d the average of guest particles, ρ_D the density of host particles, and ρ_d the density of the guest particles.

Figure 9(a) shows the TEM image of the fumed nano-alumina. In addition to the low particle diameter and a positively charged surface (Ref 26), fumed nano-alumina particles are free from pores and bear hydroxyl groups on their surface (Ref 27). Figure 9(b) shows an illustration showing the presence of positive surface charges and hydroxyl groups at the surface on the nanoparticles.

It was observed that deposition of the polymer-nano composite mixture occurred when the temperature of the gas was close to 350 °C and gas pressure was between 0.3 and 0.4 MPa in the case of Al substrate. On PP substrate, the deposition was observed at 170 °C gas temperature and 0.3-0.4 MPa gas pressure.

Coatings of 3-4- and 1-mm thicknesses were obtained on Al and PP substrates, respectively. Figure 10(a) and (b) shows the photographs of the coating obtained on Al and PP substrates, respectively.

The UHMWPE coating on Al was observed to delaminate when cut. Hence, it was subjected to a heat treatment of 200 °C for 10 min to improve the adhesion. Subsequently, the samples were cut and the cross sections were observed. Figure 11(a) and (b) shows the cross-sectional SEM/EDX images of the coating on Al and PP substrates, respectively.

The fumed nano-alumina particles played an important role in activating the UHMWPE grains by creating a network of finely dispersed particles, which bonded to the polymer surfaces.

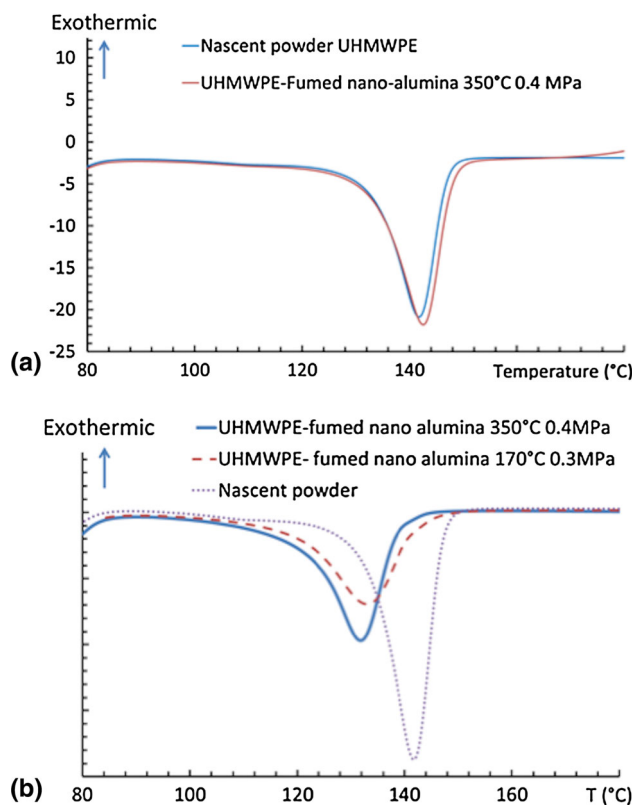


Fig. 12 (a) DSC curves of the rebounded particles at various gas temperatures. (b) DSC curves of the deposited particles

3.2 Deposition Criteria Analysis

3.2.1 Differential Scanning Calorimetry. By using DSC, it is possible to determine whether the nascent UHMWPE particles melt or not after the passage through the nozzle. Hence, the thermal state of UHMWPE particles after the impact in the cold spray process can be understood.

The DSC curves of the rebound particles were observed to have the similar melting temperature and crystallinity as that of the nascent powder. Figure 12(a) represents the DSC curves for the rebound particles. So the rebounding particles are in the nascent state.

On the other hand, the DSC curves for the deposited particles were observed to have a lower crystallinity and melting temperature than that of the nascent powder (Fig. 12b). The deposited particles were observed to melt during the cold spray experiment, and then recrystallize during the cooling.

This phenomenon is observed when UHMWPE is melt crystallized. Figure 13 shows the DSC curves of both the

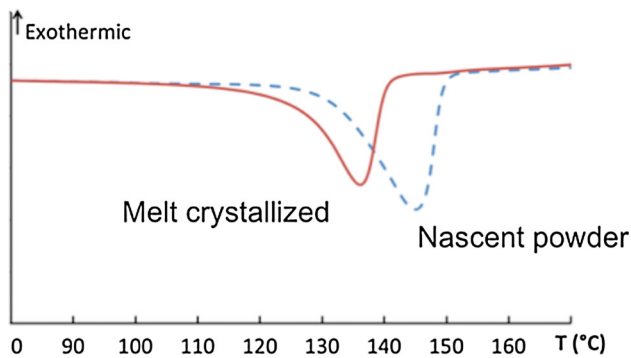


Fig. 13 DSC curves of the nascent powder and the melt-crystallized UHMWPE (Ref 30)

nascent powder and of particles crystallized from the melt UHMWPE. The much higher crystallinity and melting point are characteristics of the special structure UHMWPE nascent reactor powders (Fig. 13). The high melting temperature is attributed to the non-equilibrium chain conformations: the presence of chain-extended crystals as well as constrained chain-folded crystals (Ref 8, 28, 29).

During cold spray, the only region where the particles are heated is the nozzle region where the particles interact with the heated carrier gas. But this particle-carrier gas interaction time is extremely small. According to the DSC curves of the rebounding particles, the softening of the particles by the carrier gas has not taken place (Fig. 12a). On the other hand, the DSC curves of the deposited particles show that the UHMWPE particles have melted (Fig. 12b). Figure 14 shows an illustration of the difference in the thermal states of the rebounding particle and the depositing particle.

Finally, it is likely that in the nozzle region, the UHMWPE particles are heated enough to allow very strong ductility so that no rebound occur at the impact. It can be considered perfectly inelastic. Therefore, the kinetic energy of the particle is converted to heat and contribute to the melting of the particle. The following evaluation gives the order of magnitude of the energy required for melting a particle with 100 μm in diameter.

Evaluation of the energy required for melting one particle (100 μm of diameter):

$$\Delta E = \Delta H m X_c + m C_p \Delta T$$

with ΔH the melting enthalpy of the crystal (290 J/g), X_c the crystallinity of the nascent powder deduced from DSC (%), C_p the heat capacity (2.22 J/g/K by calculating the average of C_p between 35 and 135 $^{\circ}\text{C}$ for a material with 56% of crystallinity (Ref 31)), and m the mass of the particle which is calculated using the equation $m = \frac{4}{3} \pi r^3 d$ with d being the density of the grains (0.94 g/cm³ for the crystallinity of 0.56).

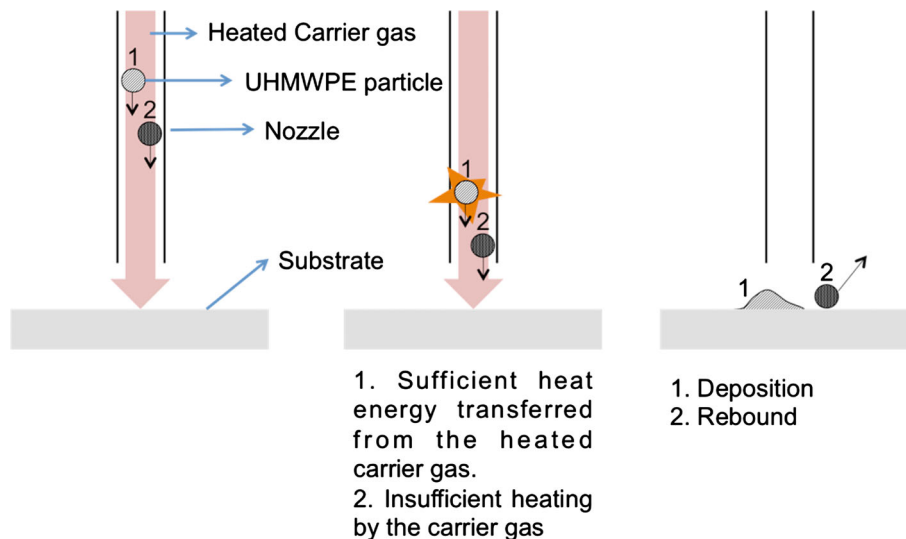


Fig. 14 Illustration of the thermal states of the rebounding and depositing particles before the impact

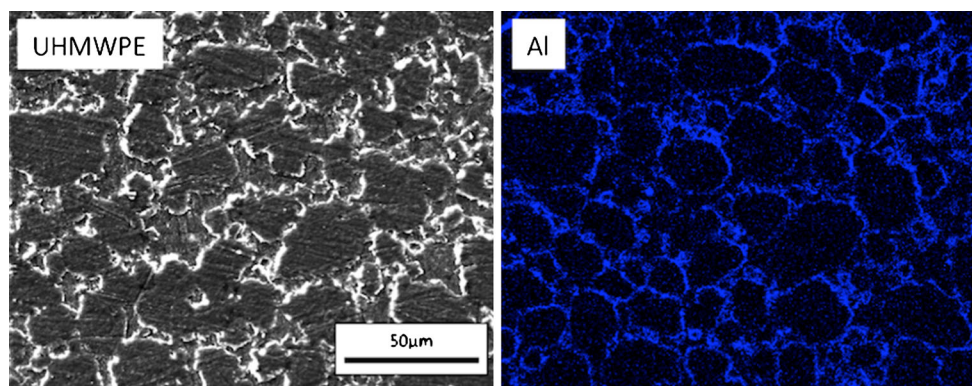


Fig. 15 SEM and EDX image of cross section of UHMWPE-fumed nano-alumina coating, respectively

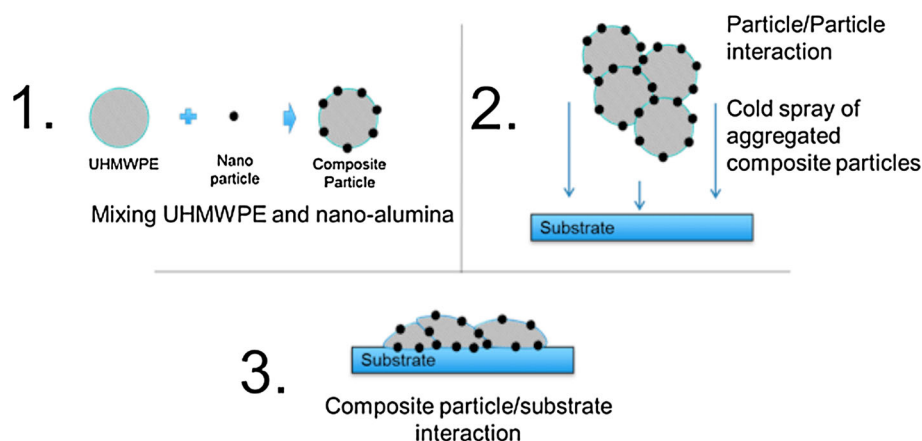


Fig. 16 Illustration of possible activation of the UHMWPE grains by the nano alumina mixing

The kinetic energy is given as follows:

$$E_c = \frac{1}{2}mV^2$$

with m the mass of the particle and V the velocity.

It is not possible to accurately measure the temperature of the particle in the end of the nozzle. For a quantitative evaluation of the energy required to melt the particle, calculation below gives the higher limit if the particle temperature in the nozzle outlet is equal to the melting temperature and the lower limit if the particle is at room temperature (ΔT equal to 0 and 100 °C)

$$8 \times 10^{-5} < \Delta E < 2 \times 10^{-4} (J).$$

Which is equivalent to a particle's velocity range as follows:

$$550 < V < 850 \text{ (m/s)}.$$

If we assume the particle velocity of the cold-sprayed UHMWPE to be typically a few hundred m/s, this order of magnitude is consistent with the DSC results. We can also notice that the fusion rate is independent of the particle mass in the limit where the particle velocity is considered independent of the particle mass.

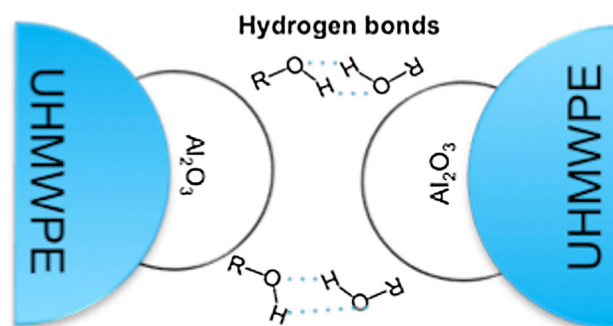


Fig. 17 Illustration of possible extra bonds introduced by hydroxyl group at the fumed nano alumina surface

3.3 Effect of the Nano-ceramic Particle

Effect of the nanoparticles in strengthening the microstructure is observed as the nanoparticles facilitated in the bonding of the UHMWPE particles together. The nanoparticles form an interconnected network at the surface of the UHMWPE particles. Figure 15 shows the SEM and its corresponding EDX image of the nano-alumina particles settled around the UHMWPE grains.

Nano-ceramic addition must have definitely increased the hardness of the coating. But as the percentage added to the feedstock is very low (4%), it is not expected to increase drastically. Additionally, it is difficult to compare with the coating without the nanoparticle addition, as the coating obtained was extremely thin and fragile to be observed.

Nano-ceramic particles act as a bond between the polymeric grains due to the hydroxyl groups at the surface of the nanoparticles. The observance of a thick-layered coating can be attributed to the presence of the nanoparticles on the grain surface. Figure 16 shows a simple illustration of the possible activation of the polymer grains by the nano-alumina particles. Nano-ceramic particles settled along the grains of the UHMWPE particles, after the mixing, form a composite particle. The composite particles are then cold sprayed on to the desired substrate. The particle/particle interaction takes place during the passage of the composite particles along the nozzle length creating an aggregate of the composite particles. This aggregation is permitted by the presence of nano-alumina particles.

Furthermore, the hydroxyl groups at the surface of the fumed nano-alumina particle (Ref 27) may also play an important role in introducing new bonds like hydrogen bonds between the polymeric grains although it is difficult to confirm until future experiments are performed. The presence of such bonds can reinforce the UHMWPE particle-particle bonding. Improvement in deposition was also observed when UHMWPE was sprayed with fumed nano silica (which also has hydroxyl groups on its surface (Ref 27)) added to the feedstock (Ref 32). Figure 17 shows a simple illustration of the possibility of the introduction of extra bonds like hydrogen bonding between the polymer grains.

4. Conclusion

This study analyzes the development of UHMWPE coatings, which is a high molecular counterpart of conventional polyethylene. The current study showed that the cold spray could be used as a low cost, and speedy technique for deposition of UHMWPE coatings with nano-alumina particles on different substrates. Following conclusions can be drawn from the experiments conducted.

Few millimeters thick coatings of UHMWPE were achieved on Al and PP substrates with the addition of fumed nano-alumina and with the incorporation of longer nozzle. A step at the center of the nozzle helped in decelerating particle flow and increasing static gas temperature. The increase of the temperature of the polymeric particles leads to softening and facilitates the bonding during the impact.

Finally, the addition of fumed nano-alumina to the feedstock UHMWPE, has contributed in effectively building up the coating thickness probably by creating bridge bonds between UHMWPE particles. Nanoparticles

created a network of finely dispersed particles, which were bonded to the polymer matrix. The types of bonds acting between the nanoparticles and the UHMWPE are unclear, although most probably are hydrogen bonds. The presence of hydroxyl groups at the surface of the fumed nano-alumina particles may have assisted in reinforcing the UHMWPE particle-particle bonding in the form of hydrogen bonds. However, the complete understanding of the deposition mechanism requires further works which are already ongoing.

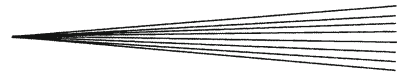
This research work is intended to reveal the possibility of coating UHMWPE by cold spray technique. This is the first step of a larger study. Hence, further studies especially the mechanical properties of the coatings would be carried out in the future.

Acknowledgments

The authors are indebted to Ticona (Oberhausen, Germany) for the generous supply of the UHMWPE sample together with its molecular characteristics. One of us, Tiana Deplancke acknowledges ONR (USA) for its financial support through the NICOP project. Authors would also like to thank JTSS internship program for financing and supporting the internship, carried out at Iwate Industrial Research Institute. This work was partly supported by the JSPS Core-to-Core Program, A. Advanced Research Networks, "International research core on smart layered materials and structures for energy saving." Authors would also like to thank Prof. Hidemasa Takana from Institute of Fluid Science (Tohoku University) for his valuable insights to understanding the flow dynamics within the nozzles.

References

1. S.P. Sitaram, J.O. Stoffer, and T.J. O'Keefe, Application of Conducting Polymers in Corrosion Protection, *J. Coat. Technol.*, 1997, **69**(866), p 65-69
2. Y.Q. Wang, L.P. Huang, W.L. Liu, and J. Li, The Blast Erosion Behaviour of Ultrahigh Molecular Weight Polyethylene, *Wear*, 1998, **218**(1), p 128-133
3. L.L. Lin, T.H. Ho, and C.S. Wang, Synthesis of Novel Trifunctional Epoxy Resins and Their Modification with Polydimethylsiloxane for Electronic Application, *Polymer*, 1997, **38**(8), p 1997-2003
4. G. Scott, *Polymers and the Environment*, Royal Society of Chemistry, Cambridge, 1999
5. A.G. Mikos, G. Sarakinos, J.P. Vacanti, R.S. Langer, and L.G. Cima, U.S. Patent No. 5,514,378, U.S. Patent and Trademark Office, Washington, DC, 1996
6. S.M. Kurtz, *The UHMWPE Handbook: Ultra-High Molecular Weight Polyethylene in Total Joint Replacement*, Academic Press, New York, 2004
7. D.C. Prevorsek, Y.D. Kwon, and H.B. Chin, Analysis of the Temperature Rise in the Projectile and Extended Chain Polyethylene Fiber Composite Armor During Ballistic Impact and Penetration, *Polym. Eng. Sci.*, 1994, **34**(2), p 141-152
8. T. Deplancke, O. Lame, F. Rousset, I. Aguilu, R. Seguela, and G. Vigier, Diffusion Versus CocrySTALLIZATION of Very Long Polymer Chains at Interfaces: Experimental Study of Sintering of UHMWPE Nascent Powder, *Macromolecules*, 2013, **47**(1), p 197-207



9. A. Papyrin, Cold Spray Technology, *Adv. Mater. Process.*, 2001, **159**(9), p 49-51
10. R.C. Dykhuizen and M.F. Smith, Gas Dynamic Principles of Cold Spray, *J. Therm. Spray Technol.*, 1998, **7**(2), p 205-212
11. V.F. Kosarev, S.V. Klinkov, A.P. Alkhimov, and A.N. Papyrin, On Some Aspects of Gas Dynamics of the Cold Spray Process, *J. Therm. Spray Technol.*, 2003, **12**(2), p 265-281
12. M. Grujicic, C.L. Zhao, C. Tong, W.S. DeRosset, and D. Helfritsch, Analysis of the Impact Velocity of Powder Particles in the Cold-Gas Dynamic-Spray Process, *Mater. Sci. Eng. A*, 2004, **368**(1), p 222-230
13. S.L. Coguill, S.L. Galbraith, D.L. Tuss, M. Ivosevic, and L.C. Farrar, U.S. Patent Application 13/506, 215, 2012
14. Y. Xu and I.M. Hutchings, Cold Spray Deposition of Thermoplastic Powder, *Surf. Coat. Technol.*, 2006, **201**(6), p 3044-3050
15. E. Leivo, T. Wilenius, T. Kinos, P. Vuoristo, and T. Mäntylä, Properties of Thermally Sprayed Fluoropolymer PVDF, ECTFE, PFA and FEP Coatings, *Prog. Org. Coat.*, 2004, **49**(1), p 69-73
16. G. Zhang, W.Y. Li, M. Cherigui, C. Zhang, H. Liao, J.M. Bordes, and C. Coddet, Structures and Tribological Performances of PEEK (Poly-Ether-Ether-Ketone)-Based Coatings Designed for Tribological Application, *Prog. Org. Coat.*, 2007, **60**(1), p 39-44
17. C.R. Lima, N.F. de Souza, and F. Camargo, Study of Wear and Corrosion Performance of Thermal Sprayed Engineering Polymers, *Surf. Coat. Technol.*, 2013, **220**, p 140-143
18. H. Assadi, F. Gärtner, T. Stoltenhoff, and H. Kreye, Bonding Mechanism in Cold Gas Spraying, *Acta Mater.*, 2003, **51**(15), p 4379-4394
19. Z. Bartczak, P.F. Beris, K. Wasilewski, A. Galeski, and P.J. Lemstra, Deformation of the Ultra High Molecular Weight Polyethylene Melt in the Plane-Strain Compression, *J. Appl. Polym. Sci.*, 2012, **125**(6), p 4155-4168
20. A.S. Alhulaifi, G.A. Buck, and W.J. Arbegast, Numerical and Experimental Investigation of Cold Spray Gas Dynamic Effects for Polymer Coating, *J. Therm. Spray Technol.*, 2012, **21**(5), p 852-862
21. A.M. Wrobel, M. Kryszewski, W. Rakowski, M. Okoniewski, and Z. Kubacki, Effect of Plasma Treatment on Surface Structure and Properties of Polyester Fabric, *Polymer*, 1978, **19**(8), p 908-912
22. P. Bhimaraj, D. Burris, W.G. Sawyer, C.G. Toney, R.W. Siegel, and L.S. Schadler, Tribological Investigation of the Effects of Particle Size, Loading and Crystallinity on Poly (Ethylene) Terephthalate Nanocomposites, *Wear*, 2008, **264**(7), p 632-637
23. C. Liu, L. Ren, R.D. Arnell, and J. Tong, Abrasive Wear Behavior of Particle Reinforced Ultrahigh Molecular Weight Polyethylene Composites, *Wear*, 1999, **225**, p 199-204
24. E. Kontou and M. Niaounakis, Thermo-mechanical Properties of LLDPE/SiO₂ Nanocomposites, *Polymer*, 2006, **47**(4), p 1267-1280
25. J. Yang, A. Sliva, A. Banerjee, R.N. Dave, and R. Pfeffer, Dry Particle Coating for Improving the Flowability of Cohesive Powders, *Powder Technol.*, 2005, **158**(1), p 21-33
26. Technical Information, Degussa AG, Frankfurt, TI 1283
27. W. Lortz, G. Perlet, W. Will, and S. Reitz, U.S. Patent No. 7,834,076, U.S. Patent and Trademark Office, Washington, DC, 2010
28. H.D. Chanzy, E. Bonjour, and R.H. Marchessault, Nascent Structures During the Polymerization of Ethylene, *Colloid Polym. Sci.*, 1974, **252**(1), p 8-14
29. S. Rastogi, D.R. Lippits, G.W. Peters, R. Graf, Y. Yao, and H.W. Spiess, Heterogeneity in Polymer Melts from Melting of Polymer Crystals, *Nat. Mater.*, 2005, **4**(8), p 635-641
30. D. Jauffrès, O. Lame, G. Vigier, and F. Doré, How Nascent Structure of Semicrystalline Polymer Powders Enhances Bulk Mechanical Properties, *Macromolecules*, 2008, **41**(24), p 9793-9801
31. J. Brandrup, E.H. Immergut, A. Abe, and D.R. Bloch, Ed., *Polymer Handbook*, Vol. 89, Wiley, New York, 1999
32. K. Ravi, Y. Ichikawa, O. Ogawa, T. Deplanke, O. Lame, and J.Y. Cavaille, Mechanistic Study and Characterization of Cold Sprayed Ultra High Molecular Weight Polyethylene-Nano Ceramic Composite Coating, *International Thermal Spray Conference and Exposition (ITSC)*, ASM, Materials Park, 2015